Biosensors and Bioelectronics 155 (2020) 112108

Contents lists available at ScienceDirect

Biosensors and Bioelectronics

journal homepage: http://www.elsevier.com/locate/bios

Gold-microrods/Pd-nanoparticles/polyaniline-nanocomposite-interface as a peroxidase-mimic for sensitive detection of tropomyosin

Azureen Mohamad [a], Mohammad Rizwan [a,b], Natasha Ann Keasberry [a], Anh Son Nguyen [c,d], Tran Dai Lam [c,d], Minhaz Uddin Ahmed [a,*]

[a] Biosensors and Biotechnology Laboratory, Chemical Science Programme, Faculty of Science, Universiti Brunei Darussalam, Jalan Tungku Link, Gadong, BE 1410, Brunei Darussalam
[b] School of Natural Sciences, Bangor University, Bangor, Gwynedd, LL57 2DG, Wales, United Kingdom
[c] Institute for Tropical Technology, Vietnam Academy of Science and Technology, 18 Hoang Quoc Viet, Hanoi, Viet Nam
[d] Graduate University of Science and Technology, Vietnam Academy of Science and Technology, 18 Hoang Quoc Viet, Hanoi, Viet Nam

ARTICLE INFO

Keywords:
Label-free food biosensor
Electrochemical detection
Peroxidase-mimic
Tropomyosin
Seafood allergens
Nanocomposite-interface

ABSTRACT

In this study, Gold-microrods (AuMRs), Pd-nanoparticles (PdNPs), and Polyaniline (PANI) nanocomposite-interface was fabricated on the screen-printed carbon-microelectrode (SPE). Each layer of the interface was characterised using field emission-scanning electron microscopy (FE-SEM) and cyclic voltammetry (CV). The fabricated SPE/AuMRs/PdNPs/PANI interface demonstrated the highest electronic current and showed excellent peroxidase-mimic towards H_2O_2 using chronoamperometry (CA). Furthermore, the SPE/AuMRs/PdNPs/PANI interface was utilised for the construction of a highly sensitive label-free electrochemical biosensor for the detection of Tpm in seafood samples. Label-free electrochemical detection of the Tpm was performed using both CA and differential pulse voltammetry (DPV) techniques. Preliminary data showed that both methods could detect Tpm as low as 0.01 pg/mL. Moreover, the developed biosensor for the detection of Tpm demonstrated excellent selectivity, high reproducibility and longer stability with an evident potential to detect Tpm in real seafood samples.

1. Introduction

Currently, to meet the food demand, global consumption of seafood has drastically increased. This has also risen the incidences of allergy caused by the seafood in allergic consumers. Therefore, the development of highly sensitive methods to detect tropomyosin (Tpm), a major common allergenic protein found in shellfish, is important. In seafood allergies, the allergen Tropomyosin (Tpm) has been identified as a common triggering protein that induces the immune reaction (Ishikawa et al., 1998; Lopata et al., 1997; Suma et al., 2007). Furthermore, according to Huang et al. and Liu et al. Tpm is relatively resistant to peptic acidic digestion, thus prolonging the effect of the protein in the system (Huang et al., 2010; Liu et al., 2011).

Tpm is an actin-binding protein that plays a role in muscle contraction, cell morphology, and motility. Tpm is present in both vertebrates and invertebrates with different isoforms for different muscle anatomy such as skeletal, cardiac and smooth muscles, but absent in plants. Nonetheless, Tpm invertebrates is considered non-allergenic even though they have a similar degree of sequence and the same functionality (James et al., 2018; Sicherer and Sampson, 2018). The basis of these findings has not yet been elucidated. Epidemiology of crustacean allergy in Asia is very prominent (Lee et al., 2013; Loh and Tang, 2018). Most people who have a crustacean allergy practice strict avoidance in consuming crustacean in food. However, accidental ingestion may occur from cross-contamination, or improper labeling of seafood (Ahmed et al., 2008, 2019). Therefore, a simple and reliable sensor for the detection of the allergen is needed for seafood safety and quality control (Ahmed et al., 2016b, 2019). However, a simple method of measuring crustacean Tpm is still lacking. Currently, enzyme-linked immunosorbent assay (ELISA) and polymerase chain reaction (PCR) are commonly used in detection of Tpm. However, with ELISA, the steps towards analysis are long and tedious. Whilst with DNA-based PCR technique, the DNA extraction for analysis is lengthy, time consuming and expensive. Thus, a simple, economical and rapid label-free electrochemical seafood biosensor was constructed using gold-microrods (AuMRs), Pd-nanoparticles (PdNPs) and polyaniline (PANI) nanocomposite on

* Corresponding author.
E-mail address: minhaz.ahmed@ubd.edu.bn (M.U. Ahmed).

https://doi.org/10.1016/j.bios.2020.112108
Received 13 November 2019; Received in revised form 15 February 2020; Accepted 17 February 2020
Available online 19 February 2020

carbon-microelectrode (SPE) (SPE/AuMRs/PdNPs/PANI) interface as a peroxidase-mimic.

Among the variety of metallic nanoparticles, gold nanomaterials (AuNMs) is the most extensively studied for amplification of the electrochemical signal and nanozyme properties in biosensors due to its simple synthesis and reproducibility (Lim and Ahmed, 2016; Mohamad et al., 2018, 2019; Rizwan et al., 2019). Further among the different AuNMs, currently, AuMRs has attracted the attention of the researchers due to asymmetry in dimensions and large aspect ratio. AuMRs is a type of AuNMs with its two dimensions in 100 nm range, and one dimension in μm. This asymmetry in dimensions provides high electronic conductivity, excellent catalytic properties, and novel physiochemical features including a large aspect ratio to AuMRs (Alagiri et al., 2017). Additionally, AuMRs have a high surface area, which presents efficient electron transport and bioconjugation of detecting molecules, biocompatibility (Lee and Ha, 2017), abundant reactive sites for enzymatic reactions, and highly stable under high ionic strength environment without supplementation of stabilising agents (Castro-Longoria et al., 2011). While there is another type of gold rods having all the dimensions in the nm ranges, which known as gold-nanorods (AuNRs). AuNMs demonstrate high optical properties and is widely used for the fabrication of the surface plasmon resonance-based sensor (Huang et al., 2009). Therefore, in this work AuMRs for the electrochemical detection of Tpm, rather than AuNRs was used for the modification of electrode. However, AuNMs, suffer from low substrate affinity and lower catalytic activity compared to biological enzymes, and so do AuMRs (Mohamad et al., 2018, 2019). Recent trends show that to avoid this limitation, bimetallic or trimetallic nanomaterials have been applied in the construction of

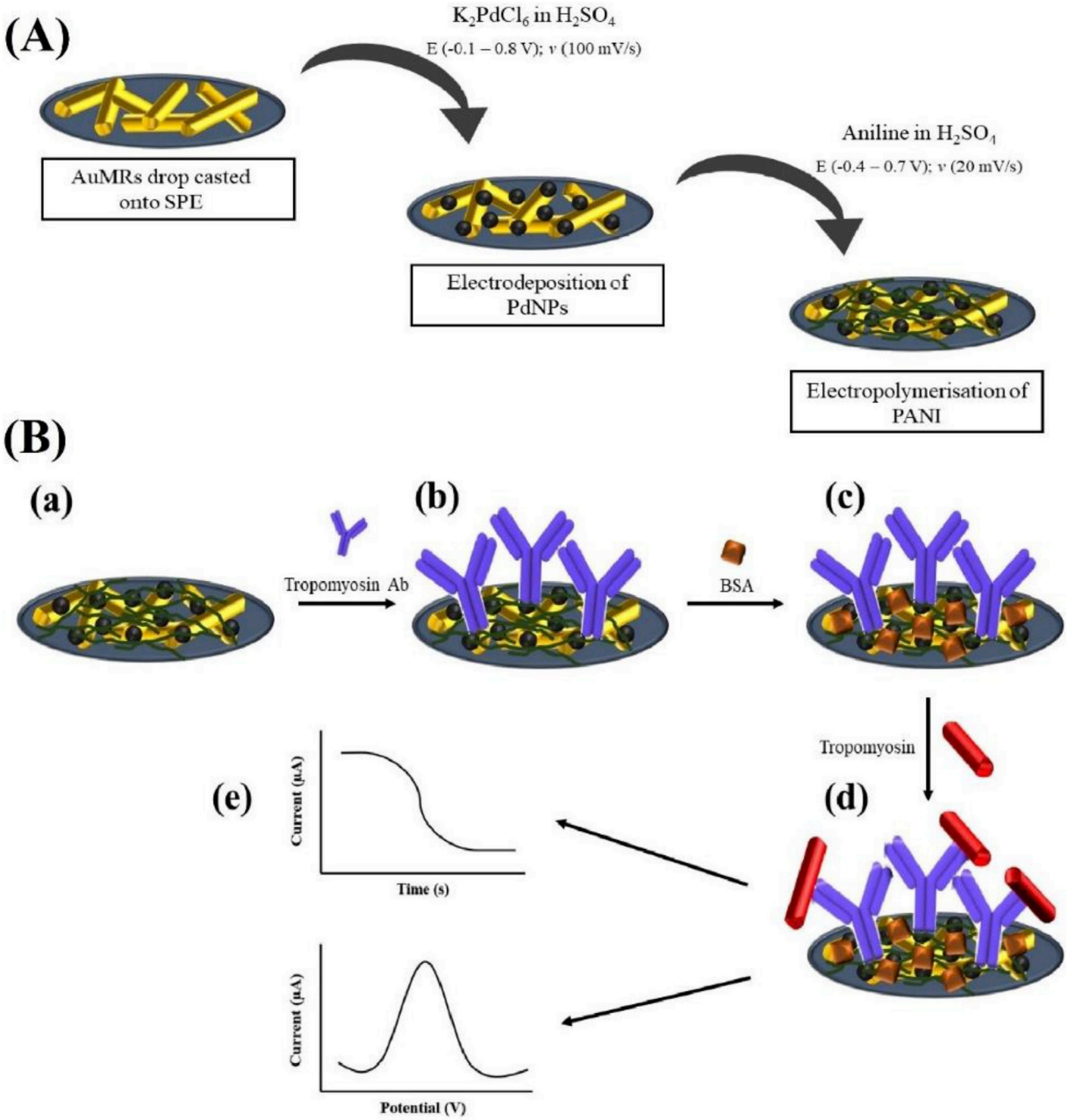

Scheme 1. Schematic of the fabrication of AuMRs/PdNPs/PANI electrode and construction of biosensor: (A) AuMRs were drop-casted onto the working electrode, followed by the electrodeposition of PdNPs, and electropolymerisation of PANI; (B) Construction of the biosensor. (a) AuMRs/PdNPs/PANI modified SPE, (b) Tpm-Ab functionalised onto the modified electrode after EDC/NHS activation, (c) Blocking of biosensor surface by BSA, (d) Introduction of different concentrations of Tpm for detection, (e) Electrochemical measurements using CA and DPV techniques.

biosensors (Ahmed et al., 2019; Mohamad et al., 2018, 2019).

A recent study shows that to achieve catalytic activity compared to biological enzymes, Palladium (Pd) has emerged as a novel alternative material. Pd is a metallic material which is well-known as a versatile catalyst in the petroleum industry, hydrogenation reaction, Suzuki coupling, and as an electrocatalyst for oxidation of primary alcohol in alkaline media (Saldan et al., 2015). Furthermore, PdNPs have been reported to carry enzyme-mimic properties i.e. as a peroxidase-mimic capable to catalyse the decomposition of hydrogen peroxide (H_2O_2) (He et al., 2010; J. Li et al., 2015a). With such ability, PdNPs could be used as an alternative to enzyme horseradish peroxidase to catalyse amplification reactions in biosensors. Therefore, intercalating PdNPs into the biosensor would further amplify the signal of detection (Lim and Ahmed, 2016).

Furthermore, current application of conducting polymers in the construction of electrochemical biosensors as an electronic transducer has abruptly risen due to its conductivity, stability, ease of preparation, and strong adherence to the electrode surface (Tomczykowa and Plonska-Brzezinska, 2019; Rizwan et al., 2019). Conducting polymers may contain π-conjugated systems that have alternating double and single chemical bonds along the polymer structure. The π-conjugation of the carbon bonds along the orientated polymer chain provides a pathway for the free movement of electrons in the polymeric structure (Ameen et al., 2013). Among the different available polymers, currently, PANI is one of the most commonly studied conductive polymers. Furthermore, PANI is an electropolymerizable polymer (Inzelt et al., 2001). Electrochemical polymerisation allows for high organisation and control of the thinness of the polymerised film on the electrode surface even on microdevices. Electropolymerisation is a simple method used to deposit conductive polymer electrochemically from monomers in the electrolyte (Ferancova and Benikova, 2012).

Therefore, in this work AuMRs, PdNPs and PANI nanocomposite-interface were fabricated on SPE to use as peroxidase-mimic for the construction of the label-free electrochemical biosensor to detect Tpm in seafood samples. To the best of our knowledge, there are no reports based on the use of AuMRs in an amperometric sensor yet. Palladium was intercalated into the material to form a bimetallic composite material to further enhance the sensing ability of the designed biosensor. Additionally, PANI was used to enhance the conductivity of the electrode surface, and protect the leaching of the AuMRs/PdNPs composite into the electrolyte during sensing. Furthermore, PANI was also employed in the fabrication to provide –NH terminals for the conjugation of the tropomyosin-antibody (Tpm-Ab) with EDC/NHS chemistry.

2. Experimental section

2.1. Chemicals

Polyclonal anti-shrimp antibody from rabbits and natural shrimp tropomyosin are both obtained from Indoor Biotechnologies (India). Chemicals such as 1-Ethyl-3-(3-dimethylaminopropyl) carbodiimide (EDC), N-hydroxysuccinimide (NHS), potassium ferrocyanide ($K_4Fe(CN)_6$), potassium ferricyanide ($K_3Fe(CN)_6$), potassium hexachloropalladate (IV) (K_2PdCl_6), sodium azide (NaN_3), bovine serum albumin (BSA) (≥98%), hydrogen peroxide solution 30% (*w/w*) in water, and gold microrods (AuMRs) colloidal suspension having diameter 200 nm and length 1000 nm were all purchased from Sigma (USA). Aniline and H_2SO_4 were purchased from Merck (USA).

The buffers used in the experiment are as follows: (1) phosphate-buffered saline (PBS) buffer for preparation of Tpm-Ab, dilutions, washing, and dissolving; (2) 0.1% NaN_3 in PBS buffer (*w/v*); (3) 5 mM H_2O_2 in PBS buffer for chronoamperometric study; (4) 5 mM $[Fe(CN)_6]^{3-/4-}$ in PBS buffer for electrochemical analysis; (5) blocking buffer, PBS buffer containing 0.1% BSA in 0.1% NaN_3 (w/v). Distilled water used in the preparations was obtained from a Millipore water purification system (18MΩ, Milli-Q, Millipore).

2.2. Instrumentation

The electrochemical experiment and analyses were carried out using cyclic voltammetry (CV), chronoamperometry (CA) and DPV techniques with an Autolab PGSTAT101 (Eco Chemie, The Netherlands) potentiostat/galvanostat linked to a desktop computer with NOVA software version 1.1.0. Disposable carbon-micro screen-printed electrode (SPE) consisting of a three-electrode system with a dimension of 1.2 × 0.3 cm was obtained from Biodevice Technology (Japan). Field-Emission Scanning Electron Microscopes (FE-SEM) to study different layers of the biosensor was done by using JEOL, JSM-7610F (Tokyo, Japan). Prior to analysis, each sample was carbon-coated for 60 s. Transmission electron microscopy (TEM) observation of AuMRs has been performed using JEOL, JEM-1400 (Tokyo, Japan). The suspension was ultrasonicated for 15 min. A drop of this suspension was placed onto a substrate and dried in air at RT for 1 h, then it was passed to secondary vacuum before realizing TEM observation.

2.3. Fabrication of AuMRs/PdNPs/PANI nanocomposite-interface

2 μL of AuMRs were drop-casted onto the working electrode and air-dried in the desiccator at room temperature. After that, electrodeposition of PdNPs was carried out as described by Li et al. (2012a,b). In brief, 10 μL of 1 mM K_2PdCl_6 in 0.5 M H_2SO_4 was dropped onto the electrode. One-cycle of cyclic voltammetry (CV) was applied between the potential range of −0.1 V to +0.8 V at 100 mV/s to electrodeposit the PdNPs onto the working electrode. The electrode was then rinsed with water and dried. Following that, PANI was electropolymerized according to Gupta and Meek (2018). Briefly, 10 mM of aniline in 0.1 M H_2SO_4 was dropped onto the electrode and 10 CV cycles were done between −0.4 V to +0.7 V at 20 mV/s to form PANI. AuMRs/PdNPs/PANI-nanocomposite -interface modified SPE was stored in the desiccator (Scheme 1A).

2.4. Construction of the biosensor

2 μL of EDC/NHS in PBS (pH 5) [1:1 (*v:v*) of 100 mM EDC and 20 mM NHS] were dropped onto the fabricated SPE/AuMRs/PdNPs/PANI electrode and allowed to react for 30 min at RT. The electrode was then washed with water and dried. After that, 2 μL of 1 μg/mL of Tpm-Ab was incubated on the working electrode to functionalise the electrode for sensing (SPE/AuMRs/PdNPs/PANI/Tpm-Ab). After 30 min, the SPE/AuMRs/PdNPs/PANI/Tpm-Ab was washed with PBS and dried. Finally, 5 μL of blocking buffer was dropped onto the SPE/AuMRs/PdNPs/PANI/Tpm-Ab and incubated for 30 min. The constructed biosensor (SPE/AuMRs/PdNPs/PANI/Tpm-Ab/BSA) was again washed, dried and stored at 4 °C until needed (Scheme 1B).

2.5. Electrochemical signal measurements

2 μL of Tpm at varying concentrations were incubated onto the working electrode for 20 min. Signal was measured using CA and DPV and the peak current heights were obtained and used for analyses. CV was carried out to study different layers of nanocomposite-interface and to characterise the electrocatalytic properties of the modified electrode. PBS buffer used in CA was purged with N_2 gas before usage. Unless otherwise stated, all measurements were made at least three times.

3. Results and discussion

3.1. Microscopic characterisation of the modified electrode

FE-SEM images of each layer of the modification of SPE were captured and compared as shown in Fig. 1. Fig. 1A shows the SEM image of the bare SPE. After AuMRs were drop-casted onto the bare working electrode, an obvious elongated shaped structure could be observed suggesting successful modification with the AuMRs (Fig. 1B). AuMRs

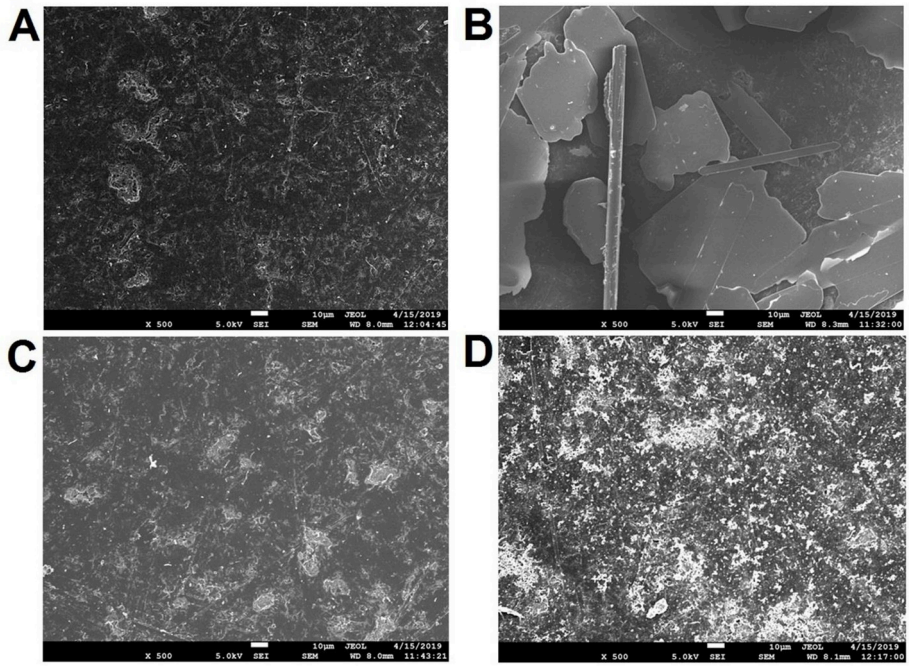

Fig. 1. FE-SEM images of the different layers on the modified SPE: (A) Bare SPE; (B) SPE/AuMRs; (C) SPE/AuMRs/PdNPs; (D) SPE/AuMRs/PdNPs/PANI.

was further characterized using TEM. TEM image demonstrated the rod shaped structures (supplementary materials Fig. S1). This portray elongated shaped structure onto the bare working electrode as AuMRs (Lee and Ha, 2017). Following the drop-casting of AuMRs, PdNPs electrodeposition was carried out on the SPE/AuMRs, and the surface topology of the SPE/AuMRs changed into an even surface, showing successful layer formation of PdNPs on the SPE/AuMRs (Fig. 1C). Finally, PANI was electrodeposited onto the SPE/AuMRs/PdNPs surface. As observed in Fig. 1D, speckles of PANI could be seen on the surface of the modified electrode, suggesting formation PANI film.

3.2. Electrochemical characterisation of modified electrode

CV was carried out to study the different layers of the modified electrode and characterised the electrocatalytic properties of surfaces at a scan rate of 20 mV/s in PBS (pH 7.4) containing 5 mM $[Fe(CN)_6]^{3-/4-}$ (Fig. 2A). After AuMRs were drop-casted onto the bare SPE, there was an obvious enhancement in current measurement on SPE/AuMRs [Fig. 2A, curve (b)] as compared to bare SPE [Fig. 2A, curve (a)]. This shows that AuMRs has enhancement properties for the electron movement between electrode-electrolyte interfaces. After PdNPs was electrodeposited onto the AuMRs-modified electrode, further enhancement of the anodic current can be seen [Fig. 2A, curve (c)]. The redox characteristics of the PdNPs enhanced the electron movements. Additionally, electrodeposition with PANI on the SPE/AuMRs/PdNPs nanocomposite-interface showed further enhancement of the redox process as shown in [Fig. 2A, curve (d)], which shows a large and broader CV compared to the bare SPE, SPE/AuMRs, and SPE/AuMRs/PdNPs. This demonstrates that electrocatalytic characteristics and electroactive surface area of the SPE/AuMRs/PdNPs/PANI were highly improved compared to bare SPE. The improved electrocatalytic activities of each of the nanomaterials and conducting polymer are consistent with results reported by Li et al. Soni et al. and Wang et al. (Li et al., 2016; Soni et al., 2019; Wang et al., 2019). With the excellent electrocatalytic characteristics and improved electroactive surface area by the hybrid nanocomposite, the biosensors could amplify signal measurement and detect very low levels of the protein of interest as well (Ahmed et al., 2019; Li et al., 2018; Lim and Ahmed, 2016).

Herein, the electrodeposition of PdNPs was carried out with one cycle of CV between −0.1 V to +0.8 V as it was adequate to be electrodeposited onto the SPE/AuMRs (Fig. 2B). A single cathodic peak can clearly be seen associated with the reduction of Pd^{2+} to Pd (Bera et al., 2004; Espino-López et al., 2019; Mukdasai et al., 2015). The subsequent cycle showed a reduced cathodic peak implying a thicker film formed on the electrode surface. Hence, only one cycle was run for the effective electrodeposition of thin film of PdNPs on the SPE/AuMRs and ensuring an enhanced electrochemical profile for the higher electrocatalytic process. Following that, PANI electropolymerisation was done on the SPE/AuMRs/PdNPs between −0.4 V to +0.7 V at 20 mV/s. As observed in Fig. 2C, the anodic and cathodic currents continuously increased with each increasing CV cycle, indicating the lengthening of the polymer. The peaks referred to the different redox states of polyaniline, representing electropolymerisation, and the doping/dedoping processes (Do et al., 2018; Guo et al., 2015).

CV was also run at various scan rates (10–100 mV/s) to investigate the electrochemical interface of the modified electrode. As shown in Fig. 2D, with increasing scan rates, the anodic current peaks shifted to a more positive potential and the cathodic current peak shifted to a more negative potential. This showed that the electron transfer between the electrode and electrolyte is almost Nernstian in a quasi-reversible electrocatalytic process. Additionally, the redox current peaks can be observed to increase with increasing scan rates. A plot of the anodic peak currents against the different scan rates can be seen showing a proportionally good linear relationship (supplementary materials Fig. S2). This shows that the SPE/AuMRs/PdNPs/PANI has a surface-controlled electron transfer mechanism (Rizwan et al., 2019).

3.3. Biocatalytical activity of SPE/AuMRs/PdNPs/PANI towards H_2O_2

For CA measurement, the SPE was immersed in 2 mL PBS (pH 6) and magnetically stirred. To find the potential of PBS, CV was carried out and the peak was measured as shown in Fig. 3A. The amperometric *i-t* curve was recorded at a potential of −0.8 V *vs* Ag/AgCl reference electrode in PBS. The current was stabilised for 60 s and 5 mM H_2O_2 was spiked. The amperometric measurement was read at 200 s. Further, biocatalytic activity of the modified electrodes was compared to the bare unmodified electrode using CA. As shown in Fig. 3B, with a bare electrode, there was only a slight catalytical effect [Fig. 3B, curve (a)], which

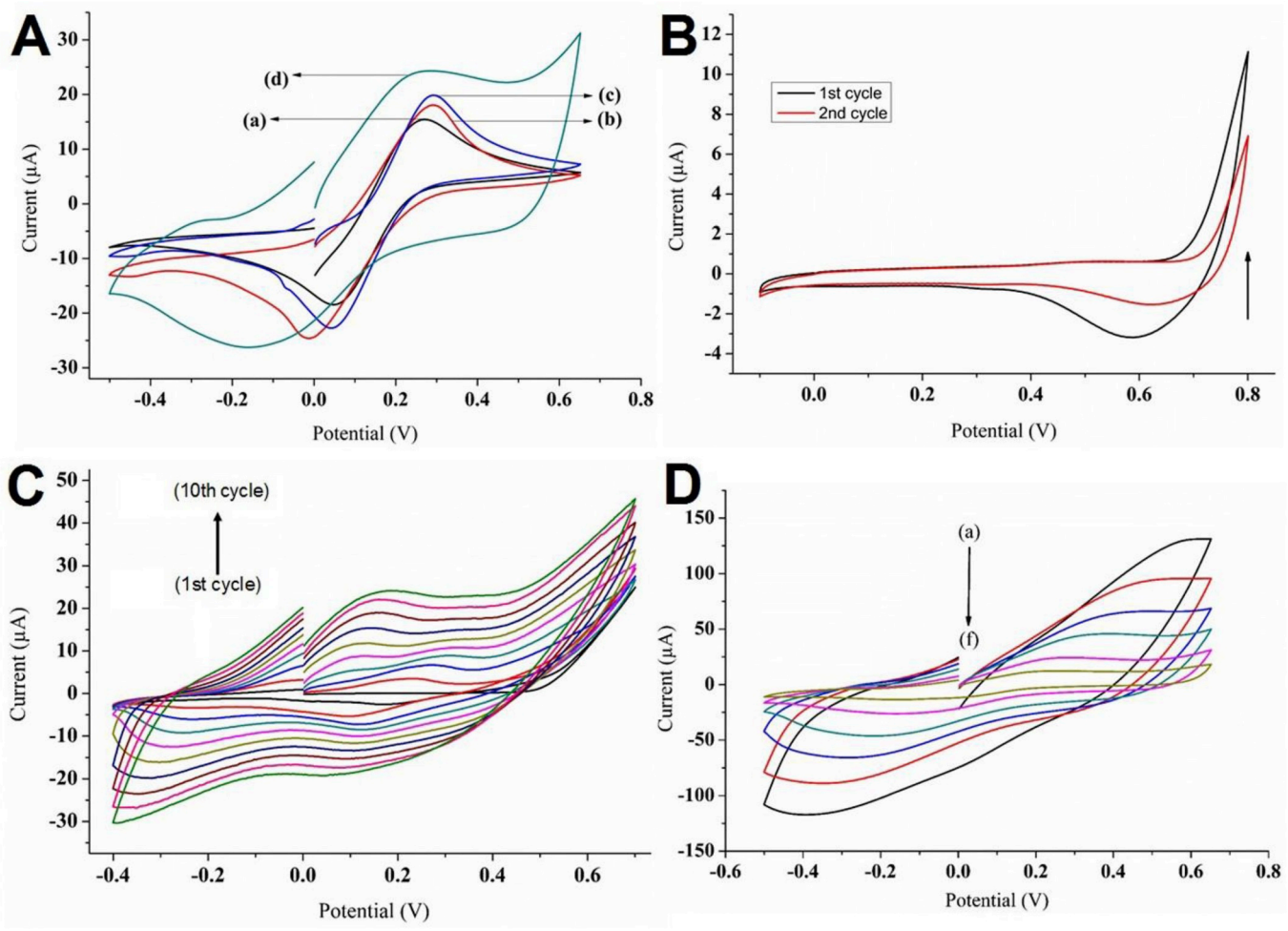

Fig. 2. Electrochemical study of modified electrode: (A) CV curves of different layers on SPE: (a) Bare SPE, (b) SPE/AuMRs, (c) SPE/AuMRs/PdNPs, and (d) SPE/AuMRs/PdNPs/PANI; (B) CV of the electrodeposition of PdNPs between −0.1 V to +0.8 V at 100 mV/s scan rate; (C) CV cycles of the electropolymerisation of PANI between −0.4 V to +0.7 V at 20 mV/s with increasing cycles; and (D) CV curves of SPE/AuMRs/PdNPs/PANI at different scan rates in $[Fe(CN)_6]^{4-/3-}$: (a) 100 mV/s, (b) 80 mV/s, (c) 60 mV/s, (d) 40 mV/s, (e) 20 mV/s, and (f) 10 mV/s.

further increases on modification with AuMRs [Fig. 3B, curve (b)], AuMRs/PdNPs [Fig. 3B, curve (c)], AuMRs/PANI [Fig. 3B, curve (d)] and demonstrated highest catalytical effect, when electrode was modified with AuMRs/PdNPs/PANI [Fig. 3B, curve (e)], as observed by large reduction in current. This reveals that the AuMRs/PdNPs/PANI could act as an excellent peroxidase-mimic towards H_2O_2 under the synergistic effect of AuMRs, PdNPs and PANI. The catalytic properties of the AuNMs, PdNPs, and PANI towards H_2O_2 are well-documented in the literature (Kafi et al., 2017; Li et al., 2012a,b, 2015a,b; Yang et al., 2017). The enhancement of the current reduction may be ascribed to the hybrid AuMRs/PdNPs/PANI as the transducer providing adsorption sites for –OH from H_2O_2 reduction. Furthermore, the large surface area of the nanomaterials might also have played a role in the electrocatalytic process, providing more active sites for the reaction (Ahmed et al., 2019; Mohamad et al., 2018, 2019).

3.4. Optimisation of parameters

Several parameters of the biosensor were optimised using CA technique to maximise the ability of the sensor. A pH study was carried out to measure the optimum catalytic ability of the SPE/AuMRs/PdNPs/PANI nanocomposite-interface towards H_2O_2. As shown in Fig. 3C, the maximum reduction current was recorded at pH 6. This is quite consistent with the study reported by Liu et al. and Yang et al. (Liu et al., 2017; Yang et al., 2017), whereby pH 6 gave the best current reduction response towards H_2O_2 for their nanocomposites containing Au, PdNPs, and PANI. Further, Tpm-Ab concentration was also optimised to maximise the sensing ability of the biosensor. Different Tpm-Ab concentrations (1, 5, and 10 μg/mL) were incubated onto the working electrode and tested to detect 10 pg/mL Tpm. As shown in supplementary materials Fig. S3, there is a decrease in reduction current as the Tpm-Ab concentration increased. This is because the increased protein layer is impeding the electron movement for the electroreduction of H_2O_2. It also implies that more Tpm-Ab was conjugated onto the surface of the electrode. The sensing towards detection of 10 pg/mL of Tpm with 1 μg/mL and 10 μg/mL of Tpm-Ab did not show a significant current difference. However, at 1 μg/mL of Tpm-Ab, a large current difference between 0 pg/mL and 10 pg/mL of Tpm was observed. Hence, 1 μg/mL of Tpm-Ab was chosen as the Tpm-Ab concentration for the maximal effect for the detection of Tpm. The reaction time between Tpm-Ab and the target protein Tpm was also optimised. As observed in supplementary materials Fig. S4, the Tpm-Ab and Tpm nearly reached its saturation point at 20 min. Thus, 20 min of reaction time was chosen for the immunocomplex formation between Tpm and Tpm-Ab.

3.5. Miniaturized protocol

The whole protocol for the biosensor construction to detect Tpm in seafood samples could be miniaturized as, AuMRs were drop-casted onto the working electrode and dried at RT, after that, electrodeposition of

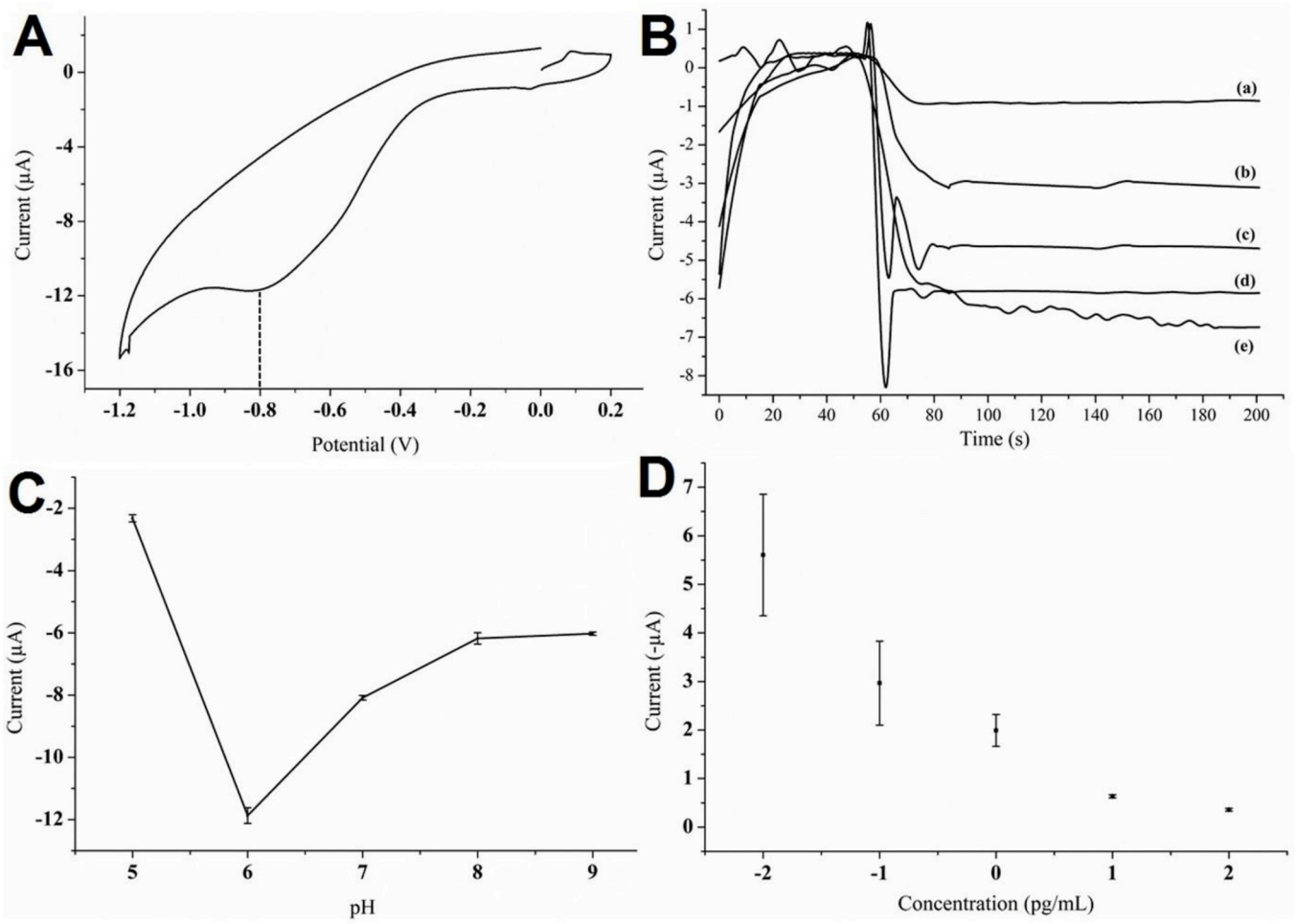

Fig. 3. Biocatalytical activity, optimisation and chronoamperometry based calibration plot study: (A) CV of PBS (pH 6) to measure the potential used for *i-t* amperometric curve measurement; (B) Amperometric *i-t* curve of (a) bare SPE, (b) SPE/AuMRs, (c) SPE/AuMRs/PdNPs, (d) SPE/AuMRs/PANI, and (e) SPE/AuMRs/PdNPs/PANI; (C) pH study of AuMRs/PdNPs/PANI nanocomposite with CA; and (D) Calibration plot of biosensor using CA in H_2O_2 to detect different concentrations of Tpm.

PdNPs and PANI was carried using CV. Fabricated SPE/AuMRs/PdNPs/PANI electrode was stored for the construction of biosensor. Subsequently, SPE/AuMRs/PdNPs/PANI electrode was activated with EDC/NHS to bind Tpm-Ab. Next blocking buffer was used for non-specific blocking and stored until to detect different concentrations of Tpm using CA and DPV.

3.6. Analytical performance using chronoamperometry technique

Under the optimal conditions, the designed biosensor was carried out to detect different concentrations of Tpm by amperometric *i-t* curve at −0.8 V in PBS (pH 6). The determination of the different concentrations of the detected Tpm was observed by the reduction current of H_2O_2. Tpm concentrations between 0.01 pg/mL to 100 pg/mL were tested. As shown in Fig. 3D, the calibration curve showed that with increasing logarithmic Tpm concentration being detected, a decrease in reduction current was observed. With more Tpm detected, more Tpm formed immunocomplexes with the Tpm-Ab. This led to the inhibition of the electron movement between the electrode surface and the electrolyte. Using the CA technique experimentally the constructed biosensor demonstrated a limit of detection of 0.01 pg/mL (Rizwan et al., 2018; Lim and Ahmed, 2015). However, as observed in Fig. 3D, using this technique the standard deviations of Tpm concentration 1, 0.1, and 0.01 pg/mL were quite large. It was hypothesised that the adsorbed O_2 from the reduction of H_2O_2 may be interfering with the electrode surface readings (Hanssen et al., 2016).

3.7. Analytical performance of biosensor using DPV

The performance of the fabricated biosensor (SPE/AuMRs/PdNPs/PANI/Tpm-Ab/BSA) was also tested using DPV with 5 mM $[Fe(CN)_6]^{3-/4-}$ in PBS (pH 7.4) between −0.1 V to +0.5 V. With increasing Tpm concentrations, the protein hindered the electron movement between the electrode surface to the electrolyte, thus, lesser $[Fe(CN)_6]^{3-/4-}$ being oxidised. Furthermore, as the protein is negatively charged in neutral pH, this would further repel the $[Fe(CN)_6]^{3-/4-}$ from the surface of the electrode. Fig. 4A shows the calibration curve of the current peak height against the logarithmic concentrations of 0.01–100 pg/mL Tpm. From the graph, it can be observed that with increasing Tpm concentrations, the current decreases and produced equation of the straight line (y = 0.66683-0.03455x) with a negative slope and 0.97261 correlation coefficient (R^2). The preliminary experimental data showed the designed biosensor measured using DPV could detect Tpm as low as 0.01 pg/mL (Rizwan et al., 2018; Lim and Ahmed, 2015).

3.8. Comparison with other Tpm assays

In this study, the designed biosensor using an antibody as bio-recognition element on SPE/AuMRs/PdNPs nanocomposite-interface fabricated on microelectrode could detect a very low concentration of

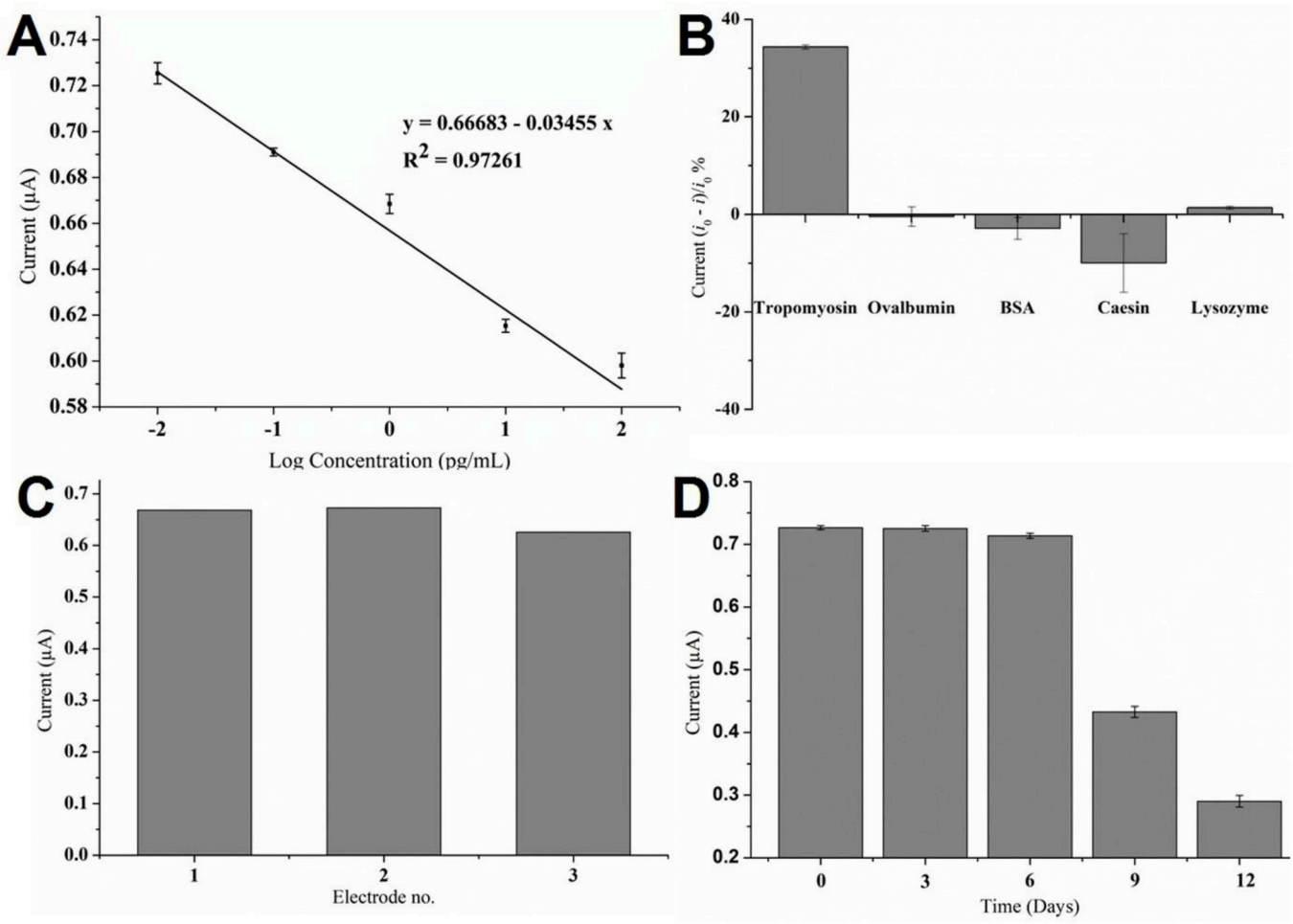

Fig. 4. Calibration plot using DPV, selectivity, reproducibility, and stability study: (A) Calibration curve of the designed biosensor against different concentrations of Tpm using DPV with $[Fe(CN)_6]^{3-/4-}$; (B) Selectivity of the designed biosensor towards the detection of Tpm against other food allergens; (C) Reproducibility of the biosensor with three different electrodes; and (D) Stability of the biosensor.

Tpm (0.01 pg/mL) both with CA and DPV techniques compared to the other assays. Other assays and techniques reported in the literature include sandwich ELISA which could detect 0.03 ng/mL (Lin et al., 2018) and 0.09 ng/mL (Zhang et al., 2014) of Tpm; aptamer as biorecognition element which could detect 0.23 ng/mL Tpm with photoelectrochemical on g-C_3N_4, TiO_2, and polyethyleneimine modified ITO electrode (Tabrizi et al., 2017), and 77 ng/mL Tpm with fluorescent (Bai et al., 2018) techniques using functionalised magnetic nanoparticles; and cell as biorecognition element which could detect 30 ng/mL Tpm using electrochemical impedance spectroscopy (Zhu et al., 2015) on fluorescent magnetic beads. Therefore, it portrayed that AuMRs/PdNPs/PANI nanocomposite-interface fabrication on SPE has successfully enhanced the sensitivity of the biosensor. Furthermore, the utilisation of the SPE played a role in the improvement of the sensing ability (Ahmed et al., 2008, 2016b, 2019). According to Orozco et al. the performance of SPE improved because increased mass transport due to radial diffusion, enhanced faradaic to capacitive current ratio, and decreased ohmic drop (Ahmed et al., 2019; Orozco et al., 2010). Additionally, SPE could be mass-produced and easily disposed (Ahmed et al., 2016a).

Table 1
Spike-and-recovery assay using the biosensor.

Dilution factor	Spiked concentration (pg/mL)	Detected concentration (pg/mL)	Recovery (%)	RSD (%)
1 000 000	0.1	0.1	110.9	5.5
	1	0.87	87.1	1.3
	10	11.6	117.6	10.3

3.9. Selectivity, reproducibility, and stability of the biosensor

The selectivity of the electrochemical biosensor was tested against other common food allergens (Ovalbumin, BSA, Casein, and Lysozyme). As shown in Fig. 4B, the biosensor was very selective towards the food allergens. The reproducibility of the electrode was also investigated as shown in Fig. 4C. 0.1 pg/mL of Tpm was incubated onto three electrodes. The relative standard deviation (RSD) between the electrodes was 3.96% showing good reproducibility. Furthermore, the stability of the modified electrode was also tested (Fig. 4D). The electrodes were stored in the refrigerator at 4 °C. The electrode showed a until the 6th day.

3.10. Application in seafood matrix

Analysis in the seafood matrix was tested in a shrimp-free cream cracker. A simple food sample refinement method was used. The sample was grounded and suspended in PBS and incubated at 60 °C for 1 h. The sample was centrifuged at 3500 rpm for 10 min, and the supernatant was collected. The supernatant was diluted to 1 000 000 dilution factor and spiked with 0.1, 1, and 10 pg/mL Tpm. The samples were detected using the designed SPE/AuMRs/PdNPs/PANI/Tpm-Ab/BSA electrochemical

biosensor. As shown in Table 1, the % recovery was between 87 – 117% with RSD ranged from 1% to 10%. The data showed quite acceptable recoveries in a complicated seafood matrix for the designed biosensor.

4. Conclusion

A highly sensitive AuMRs/PdNPs/PANI-modified microelectrode was fabricated towards the highly sensitive detection of Tpm. The AuMRs/PdNPs/PANI nanocomposite-interface was able to enhance the electrocatalytic ability of the designed biosensor. Both CA and DPV techniques were carried out to detect Tpm. Both techniques demonstrated a very low level for the sensitive detection (0.01 pg/mL) of Tpm on AuMRs/PdNPs/PANI nanocomposite-interface compared to recently reported assay in the literature (Lin et al., 2018; Tabrizi et al., 2017). Furthermore, both techniques demonstrated a 0.01–100 pg/mL range for the detection of Tpm. However, DPV analysis showed a dynamic linear range with high R^2 for the detection of different concentrations of Tpm between 0.01 to 100 pg/mL. In the future, parameters will be studied for Tpm detection using the CA technique with higher R^2. Additionally, biosensor showed excellent selectivity, high reproducibility and longer stability with an evident potential to detect Tpm in real seafood samples. Further, AuMRs/PdNPs/PANI-modified SPE could be used for the construction of biosensors to highly sensitive detection of other food allergens, such as Ovalbumin and Casein.

Funding

This work was partly supported by the Universiti Brunei Darussalam's grant UBD/RSCH/1.4/FICBF(b)/2018/010.

Declaration of competing interest

The authors declare that they have no known competing financial interests or personal relationships that could have appeared to influence the work reported in this paper.

CRediT authorship contribution statement

Azureen Mohamad: Formal analysis, Investigation, Data curation, Writing - original draft, Visualization. **Mohammad Rizwan:** Writing - review & editing. **Natasha Ann Keasberry:** Data curation, Writing - review & editing, Supervision. **Anh Son Nguyen:** Resources, Investigation. **Tran Dai Lam:** Resources, Investigation. **Minhaz Uddin Ahmed:** Conceptualization, Methodology, Validation, Resources, Data curation, Writing - review & editing, Supervision, Project administration, Funding acquisition.

Acknowledgment

Azureen Mohamad wishes to thank the Ministry of Education of Brunei Darussalam for her Ph.D. fellowship. Dr. Mohammad Rizwan gratefully acknowledge CALIN and the Welsh European Funding Office (WEFO). The authors gratefully acknowledge the associated international laboratory "Functional Composite Materials (FOCOMAT)" between France and Vietnam for the support in this work. The authors would like also to acknowledge Dr. Alessandro Pugliara (INPT-CIRIMAT, Toulouse, France) and Mr. Armel Descamps-Mandine (CNRS, Toulouse, France) for the help with the TEM experiment.

Appendix A. Supplementary data

Supplementary data to this article can be found online at https://doi.org/10.1016/j.bios.2020.112108.

References

Ahmed, M.U., Hossain, M.M., Tamiya, E., 2008. Electroanalysis 20, 616–626.
Ahmed, M.U., Hossain, M.M., Safavieh, M., Wong, Y.L., Rahman, I.A., Zourob, M., Tamiya, E., 2016a. Crit. Rev. Biotechnol. 36, 495–505.
Ahmed, M.U., Zourob, M., Tamiya, E., B, E., 2016b. Food Biosensors. Royal Society of Chemistry, UK.
Ahmed, M.U., Zourob, M., Tamiya, E., B, E., 2019. Immunosensors. Royal Society of Chemistry, UK.
Alagiri, M., Rameshkumar, P., Pandikumar, A., 2017. Microchim. Acta 184, 3069–3092.
Ameen, S., Akhtar, M.S., Song, M., Shin, H.S., 2013. Metal oxide nanomaterials, conducting polymers and their nanocomposites for solar energy. In: Morales-Acevedo, A. (Ed.), Solar Cells. IntechOpen Limited, UK, pp. 203–259.
Bai, J., Sun, M., Wu, Q., Mo, S., Zhang, Y., Wang, J., Wei, X., Zhang, J., 2018. Sensor. Actuator. B Chem. 263, 43–49.
Bera, D., Kuiry, S.C., Seal, S., 2004. J. Phys. Chem. B 108, 556–562.
Castro-Longoria, E., Vilchis-Nestor, A.R., Avalos-Borja, M., 2011. Colloids Surf. B Biointerfaces 83, 42–48.
Do, J.-S., Chang, Y.-H., Tsai, M.-L., 2018. Mater. Chem. Phys. 219, 1–12.
Espino-López, I.E., Romero-Romo, M., de Oca-Yemha, M.G.M., Morales-Gil, P., Ramírez-Silva, M.T., Mostany, J., Palomar-Pardavé, M., 2019. J. Electrochem. Soc. 166, D3205–D3211.
Ferancova, A., Benikova, K., 2012. Synthetic polymers for electrochemical DNA biosensors. In: Ozsoz, M. (Ed.), Electrochemical DNA Biosensors. Pan Stanford, Florida, pp. 331–353.
Guo, F., Ye, K., Huang, X., Gao, Y., Cheng, K., Wang, G., Cao, D., 2015. RSC Adv. 5, 94008–94015.
Gupta, S., Meek, R., 2018. Sensor. Actuator. B Chem. 274, 85–101.
Hanssen, B.L., Siraj, S., Wong, D.K.Y., 2016. Recent strategies to minimise fouling in electrochemical detection systems. Rev. Anal. Chem. 35, 1–28.
He, W., Wu, X., Liu, J., Hu, X., Zhang, K., Hou, S., Zhou, W., Xie, S., 2010. Chem. Mater. 22, 2988–2994.
Huang, X., Neretina, S., El-Sayed, M.A., 2009. Adv. Mater. 21, 4880–4910.
Huang, Y.-Y., Liu, G.-M., Cai, Q.-F., Weng, W.-Y., Maleki, S.J., Su, W.-J., Cao, M.-J., 2010. Food Chem. Toxicol. 48, 1196–1201.
Inzelt, G., Csahók, E., Kertész, V., 2001. Electrochim. Acta 46, 3955–3962.
Ishikawa, M., Ishida, M., Shimakura, K., Nagashima, Y., Shiomi, K., 1998. Biosci. Biotechnol. Biochem. 62, 1337–1343.
James, J.K., Pike, D.H., Khan, I.J., Nanda, V., 2018. Structure 26, 997–1006.
Kafi, A.K.M., Wali, Q., Jose, R., Biswas, T.K., Yusoff, M.M., 2017. Microchim. Acta 184, 4443–4450.
Lee, J., Ha, J.W., 2017. Phys. Chem. Chem. Phys. 19, 24453–24457.
Lee, A.J., Thalayasingam, M., Lee, B.W., 2013. Asia Pac. Allergy 3, 3–14.
Li, A., Zhao, X., Hou, Y., Liu, H., Wu, L., Qu, J., 2012a. Appl. Catal. B Environ. 111–112, 628–635.
Li, Z., Zhang, J., Zhou, Y., Shuang, S., Dong, C., Choi, M.M.F., 2012b. Electrochim. Acta 76, 288–291.
Li, J., Liu, W., Wu, X., Gao, X., 2015a. Biomaterials 48, 37–44.
Li, S., Xiong, J., Shen, J., Qin, Y., Li, J., Chu, F., Kong, Y., Deng, L., 2015b. J. Appl. Polym. Sci. 42409, 1–6.
Li, Y., Song, H., Zhang, L., Zuo, P., Ye, B.-C., Yao, J., Chen, W., 2016. Biosens. Bioelectron. 78, 308–314.
Li, R., Liu, L., Zhu, H., Li, Z., 2018. Anal. Chim. Acta 1008, 38–47.
Lim, S.A., Ahmed, M.U., 2015. Biosens. Bioelectron. 70, 48–53.
Lim, S.A., Ahmed, M.U., 2016. RSC Adv. 6, 24995–25014.
Lin, S.Y., Lee, C.H., Huang, E.S., Sheu, S.C., Yu, H.S., 2018. Food Anal. Methods 11, 2607–2613.
Liu, G.-M., Huang, Y.-Y., Cai, Q.-F., Weng, W.-Y., Su, W.-J., Cao, M.-J., 2011. J. Sci. Food Agric. 91, 163–170.
Liu, A., Yu, Z., Wei, M., Wang, Q., Tian, Y., Zhao, Z., Liang, J., 2017. Anal. Lett. 51, 512–522.
Loh, W., Tang, M., 2018. The epidemiology of food allergy in the global context. Int. J. Environ. Res. Publ. Health 15, 1–8.
Lopata, A.L., Zinn, C., Potter, P.C., 1997. J. Allergy Clin. Immunol. 100, 642–648.
Mohamad, A., Keasberry, N.A., Ahmed, M.U., 2018. Anal. Sci. 34, 1257–1263.
Mohamad, A., Teo, H., Keasberry, N.A., Ahmed, M.U., 2019. Crit. Rev. Biotechnol. 39, 50–66.
Mukdasai, S., Crowley, U., Pravda, M., He, X., Nesterenko, E.P., Nesterenko, P.N., Paull, B., Srijaranai, S., Glennon, J.D., Moore, E., 2015. Sensor. Actuator. B Chem. 218, 280–288.
Orozco, J., Fernández-Sánchez, C., Jiménez-Jorquera, C., 2010. Sensors 10, 475–490.
Rizwan, M., Elma, S., Lim, S.A., Ahmed, M.U., 2018. Biosens. Bioelectron. 107, 211–217.
Rizwan, M., Hazmi, M., Lim, S.A., Ahmed, M.U., 2019. J. Electroanal. Chem. 833, 462–470.
Saldan, I., Semenyuk, Y., Marchuk, I., Reshetnyak, O., 2015. J. Mater. Sci. 50, 2337–2354.
Sicherer, S.H., Sampson, H.A., 2018. J. Allergy Clin. Immunol. 141, 41–58.
Soni, A., Pandey, C.M., Pandey, M.K., Sumana, G., 2019. Anal. Chim. Acta 1055, 26–35.

Suma, Y., Ishizaki, S., Nagashima, Y., Lu, Y., Ushio, H., Shiomi, K., 2007. Comp. Biochem. Physiol. B Biochem. Mol. Biol. 147, 230–236.
Tabrizi, M.A., Shamsipur, M., Saber, R., Sarkar, S., Ebrahimi, V., 2017. Biosens. Bioelectron. 98, 113–118.
Tomczykowa, M., Plonska-Brzezinska, E.M., 2019. Polymers 11, 1–36.
Wang, L., Meng, T., Liang, L., Sun, J., Wu, S., Wang, H., Yang, X., Zhang, Y., 2019. Sensor. Actuator. B Chem. 278, 133–139.
Yang, Y., Liu, Q., Liu, Y., Cui, J., Liu, H., Wang, P., Li, Y., Chen, L., Zhao, Z., Dong, Y., 2017. Biosens. Bioelectron. 90, 31–38.
Zhang, H., Lu, Y., Ushio, H., Shiomi, K., 2014. Food Chem. 150, 151–157.
Zhu, P., Sun, X., Ji, J., Gu, W., Jiang, H., Zhang, G., Jiang, D., 2015. Biosens. Bioelectron. 70, 482–490.